Alexandros D. Sidiropoulos*, Evghenii Harea, Avraam A. Konstantinidis and Elias C. Aifantis

"Pop-in" and "pop-out" effect in monocrystalline silicon. A statistical investigation

https://doi.org/10.1515/jmbm-2017-0015

Abstract: Pop-in and pop-out effects in silicon (Si) have long been known. They were evidenced in the indentation loading-unloading curves as a sudden displacement discontinuity. They consist in a sudden contraction (pop-in) or a sudden expansion (pop-out) of the material underneath the indenter in a short period of time and are attributed to Si phase transformations that take place during the nanoindentation procedure. In this paper, first we provide a statistic analysis of such pop-in/pop-out events depending on the maximum indentation load and second we examine the dependence of their appearance on the indentation loading-unloading rate.

Keywords: nanoindentation; pop-in; pop-out; Tsallis *q*-statistics.

1 Introduction

Monocrystalline silicon (mono-Si) or single-crystal Si is the main material used for solid-state electronics and infrared optical technologies. It consists of a Si crystal lattice spanning continuously the specimen to its ends, with no grain boundaries. In its amorphous counterpart, there is limited atomic order and in a small scale only. Between these two extremes, there is polycrystalline silicon, which consists of a cluster of small crystals on crystallites. Mono-Si is prepared from very pure silicon only. It can be alloyed with small amounts of other elements added to alter in a controlled manner its semiconducting properties. Most silicon single crystals are grown by the Czochralski method [1], they are fabricated into cylindrical ingots up to 2 m in length and 45 cm in diameter, which are subsequently cut into thin slices, resulting to wafers on which the chips are manufactured. Over the few last decades, mono-Si became the most important material in technology and science. Its availability and relatively low cost are the main reasons for its use in the development of electronic devices, and associated revolution in electronics and IT sectors [2] ("era of silicon").

High-pressure studies showed that monocrystalline silicon exhibits a phase transformation for pressures ranging between 9 and 16 GPa. Cubic diamond (Si-I) phase is transformed into a metallic structure b-tin (Si-II) [3, 4]. This phenomenon is accompanied with a densification (volume contraction) of about 20%. Experiments also indicate that the first phase formed from Si-II in 10–12 GPa, under slow decompression, was Si-XII (or R8-rhombohedral structure with eight atoms per unit cell), leading to a 9% expansion of material [5, 6]. As the material is further decompressed, the degree of rhombohedral distortion gradually decreases and a mixture of Si-XII and Si-III phases is produced (bc8-body centered cubic structure with 16 individuals per unit cell), whereas the Si-XII remains at ambient pressure.

Nanoindentation experiments in monocrystalline silicon [7–16] showed a similar behavior in the phase transformation mechanisms that occur, but with small differences in the transformation paths. More specifically, silicon follows different paths during the indentation unloading stage, with Si-II producing mainly amorphous material (a-Si) under rapid unloading, and a mixture of Si-III and Si-XII only when there is sufficient time for nucleation of these crystalline phases. These phase transformations result in sudden/discontinuous deformation phenomena under the tip of the indenter. One phenomenon is the densification of the material underneath the indenter, which manifests itself in the indentation loading curve through a sudden displacement discontinuity called pop-in. Another phenomenon is a sudden material expansion that occurs during nanoindentation in the unloading curve, and also manifests itself as a displacement discontinuity, called pop-out.

In this work, we provide a statistical analysis pertaining to the occurrence of these phenomena. The external parameters that we vary are the maximum indentation load and the loading rate. Our experimental data were statistically analyzed by using a Tsallis q-distribution [17] which is a suitable method for extracting microstructure information for systems far from thermodynamic equilibrium exhibiting strong randomness and heterogeneity,

***Corresponding author: Alexandros D. Sidiropoulos,** Aristotle University of Thessaloniki, Thessaloniki 54124, Greece, e-mail: alexandersid13@gmail.com
Evghenii Harea: Institute of Sciences, Academy of Sciences of Moldova, Chisinau, Moldova
Avraam A. Konstantinidis: Aristotle University of Thessaloniki, Thessaloniki 54124, Greece
Elias C. Aifantis: Aristotle University of Thessaloniki, Thessaloniki 54124, Greece; ITMO University, St. Petersburg 197101, Russia; and Togliatti State University, Togliatti 445020, Russia

for which Boltzmann-Gibbs statistics and corresponding power laws do not suffice to model material behavior.

2 Experimental procedure

2.1 Specimen preparation and investigation methods

The nanoindentation tests were performed using p-type single-crystal silicon wafers with an (100) orientation. The wafer that was doped with boron had a resistance of 5 Ohm/cm^2. Monocrystals were grown by the Czochralski process into ingots of 1 m in length. These cylinders are then sliced into thin wafers of 0.5 mm thickness for further processing. The wafers finally were subjected to chemo-mechanical polishing.

The nanoindentation tests were performed at room temperature in air. The specimens were tested using a nanoindenter CSM Instruments SA nanohardness tester (NHT) with a trihedral diamond pyramid (Berkovich) tip with a radius of 20 nm. The determination of the hardness and Young’s modulus were established from the nano/microindentation curves by using the Oliver-Pharr method [18, 19]. To acquire the images of the imprints a LEICA DM2500M Microscope was used with a 100× magnification.

2.2 First experimental phase

In the first phase of the investigation, we made a statistical analysis of the presence of pop-in and pop-out effects, in monocrystalline Si wafers according to the maximum indentation load. The thickness of the Si wafers was 0.5 mm. The maximum applied load (Pmax) was varied between 50 and 200 mN. Twenty indents with trapezoidal loading were performed for each load. Some samples (i.e. polymers, etc.) exhibit creep, such that under constant load, an increased normal displacement will be observed. This phenomenon will affect the slope of the unloading curve and the maximum penetration, resulting in incorrect calculations of H and Er. In order to avoid these miscalculations, a ‘hold’ (holding time) at peak load segment is added to the load profile, yielding a trapezoidal loading function (Figure 1). The duration of this hold segment can be determined by experimental methods such that a maximum penetration depth is reached prior to unloading. Thus, the unloading curve and the maximum depth will be accurate, resulting in more accurate material property calculations.

All measurements on the silicon wafers were conducted in the (100) crystallographic plane. The

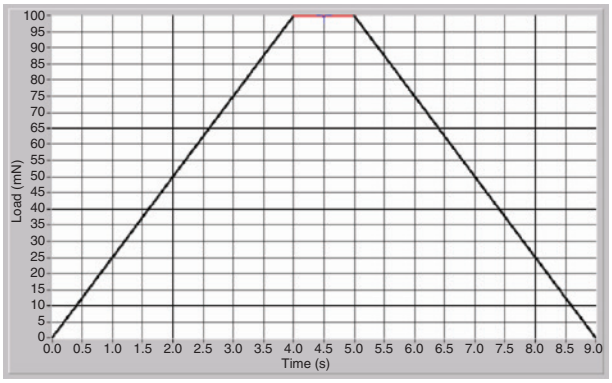

Figure 1: Load versus time curve, illustration of trapezoidal sequence.

Table 1: Experimental parameters.

Indents per load	Maximum load	Loading/unloading rate	Holding time
20	50 mN	80 mN/min	15 s
20	100 mN	80 mN/min	15 s
20	150 mN	80 mN/min	15 s
20	200 mN	80 mN/min	15 s

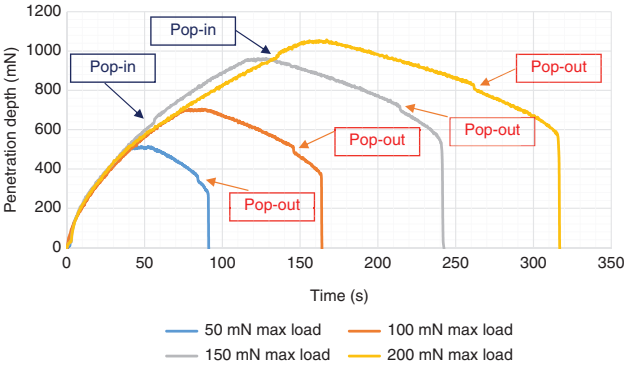

Figure 2: Penetration depth versus time curves of silicon wafers for four different loads, from 50 mN to 200 mN.

indentation loading and unloading rate was 80 mN/min and the holding time was 15 s. In Table 1, someone can see the experimental parameters for the four different loads.

Indicative displacement/penetration versus time curves, as well as load versus displacement curves for four different indentation maximum loads ranging from 50 mN to 200 mN, are shown in Figures 2 and 3, respectively.

In Figure 2, the occurence of sudden discontinuities in the loading curves of silicon wafers for higher maximum loads of 150 mN and 200 mN is shown with arrows (blue arrows). For a load of 150 mN the

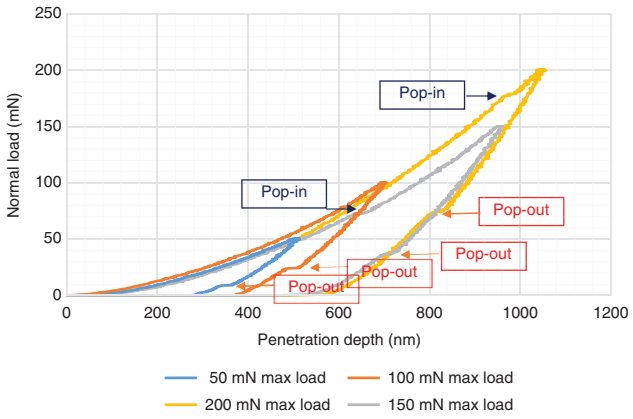

Figure 3: Normal load versus penetration depth curves of silicon wafers for four different loads, from 50 mN to 200 mN.

discontiunity appeared at about 640 nm penetration depth, 60 s after the beginning of the experiment. In the 200 mN curve the discontiunity appeared at about 950 nm penetration depth, almost 135 s after the experiment has began. On the other hand, sudden discontinuities were observed in all four curves in the unloading stage of indentation (red arrows). For a 50 mN load, a discontinuity appeared at 350 nm penetration depth, 85 s after the beginning of the test, for a 100 mN load at 510 nm penetration depth after 145 s; for a 150 mN load at 710 nm penetration depth at 210 s; and finally for a load at 200 mN at 810 nm penetration depth after 260 s. All these discontinuities indicate the apperance of pop-in and pop-out effects, a hypothesis that is also confirmed by observing the load-displacement curves (Figure 3).

Figure 3 illustrates the load versus depth curves for the four different loads. Discontinuities in this case manifest as sudden steps in the curves in both loading and unloading stages. These discontinuities are known in the literature as pop-ins and pop-outs.

In Figure 4, optical images of the four indentation imprints on silicon wafers for loads from 50 to 200 mN are illustrated. The first image shows no cracks for the silicon substrate for a load of 50 mN, while in the next image for a load of 100 mN the creation of radial cracks from the three corners of the indentation impression can be seen. For higher loads of 150–200 mN radial cracks extend while median cracks and lateral cracks appear, causing uplift of the sides of the imprint and large flakes of material are also visible at one corner of the indentation.

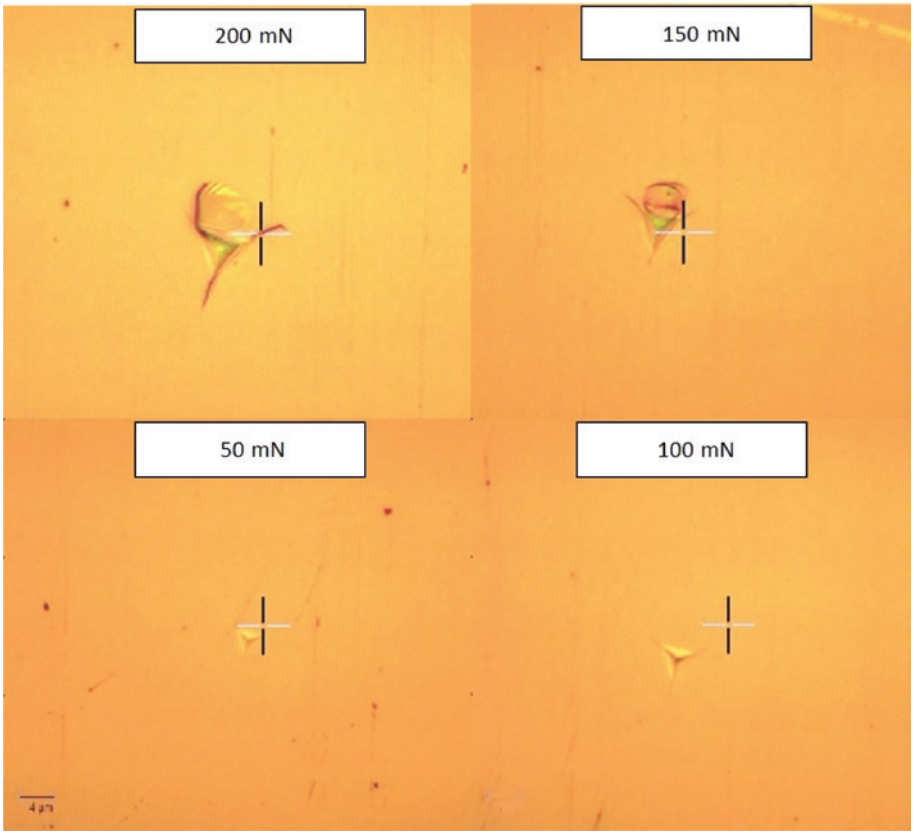

Figure 4: Optical images of the four indentation imprints on silicon wafers for maximum loads from 50 to 200 mN.

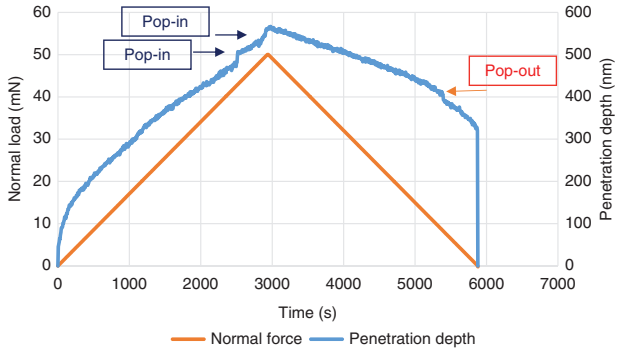

Figure 5: Normal load versus time and penetration depth versus time curves of silicon wafer for low loading/unloading rate (1 mN/min).

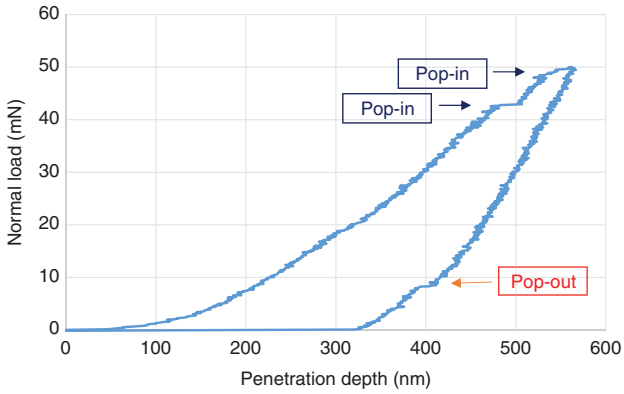

Figure 6: Normal load versus penetration depth curve of silicon wafer for low loading/unloading rate (1 mN/min).

2.3 Second experimental phase

In the second phase of the investigation, experiments with very low loading/unloading rate (from 80 mN/min reduced to 1 mN/min) were conducted. The maximum load kept the same as in Experiment 1 at 50 mN. The results of this experiment were compared with those of Experiment 1, in order to reach conclusions regarding the dependence of appearance of pop-ins and pop-outs on the indentation loading/unloading rate. During the experiment 20 imprints were made. The experiment was performed with trapezoidal sequence and holding time 15 s, between loading and unloading stage.

In Figures 5 and 6 sudden discontinuities were observed in both loading and unloading stages of the indentation process, revealing the occurrence of the pop-in (blue arrows) and pop-out (red arrows) effects. In a total of 20 experiments, 15 pop-ins and 17 pop-outs were counted.

3 Results

Table 2 shows the total number of occurrences of pop-ins and pop-outs per experiment. In the first experiment for a 50 mN max load, the amount of pop-ins was zero, while pop-outs appeared 16 times. The second experiment for 100 mN showed the same results, with the amount of pop-ins being zero and the amount of pop-outs reaching 20. For higher loads of 150 and 200 mN the first pop-ins appear. Four pop-ins were counted in the third experiment and six in the fourth. On the other hand the sum of the pop-outs remained almost the same, with 19 occurrences in the third experiment and 17 in the fourth.

It is obvious that the number of pop-outs in all four experiments remains almost the same with an average value of about ≈90% in the total amount of the imprints. On the other hand, the number of pop-ins increases by increasing the maximum indentation load, as shown in Figure 7 below.

As it is clear from Figure 7, the appearance of pop-ins is strongly dependent on the maximum indentation load. On the other hand, despite the fact that pop-out events are also connected strongly with the maximum indentation load, we can infer that for loads between 50 mN and 200 mN, the transformation of Si-II to crystalline phases Si-III and Si-XII takes place almost in all the cases; resulting in no significant changes in the number of pop-out events.

The probability distribution $p(s)$ of the pop out size is illustrated in Figure 8 where the observed data are fitted with Tsallis q-Gaussian distribution, given by the following equation

$$p(s) = [1-(1-q)bs^2]^{\frac{1}{1-q}} \quad (1)$$

where q is the Tsallis entropic index and b is a constant. The index q is a measure of system's non extensivity and shows the deviation from the standard Boltzmann-Gibbs entropy. The values of q and b were found equal to 1.5 and 1.8, respectively. These values are in good agreement with the values obtained in literature for the study of complex systems with fractality and disorder [20–23]. In Figure 7 we also illustrate the q-Gaussian for $q = 1.65$ and the Gaussian case (dashed line). For the case of $q = 1.65$ a longer tail is observed and the distribution is starting to behave (decrease) like a power law for larger pop-out sizes. This value has already appeared [24, 25] (as one of the q's of the corresponding q-triplet) at the edge of chaos of the logistic map. Since strong chaos is recovered for $q = 1$, which corresponds to a positive Lyapunov exponent [22], the q value of 1.5 obtained from the optimum fitting of our data indicates the weakly chaotic behavior of our system.

Table 2: Table summarizing the appearance of pop-ins and pop-outs, in monocrystalline silicon for different loads between 50 and 200 mN.

Indent number	50 mN max load		100 mN max load		150 mN max load		200 mN max load	
	Pop-ins	Pop-outs	Pop-ins	Pop-outs	Pop-ins	Pop-outs	Pop-ins	Pop-outs
1	–	✓	–	✓	–	✓	–	✓
2	–	✓	–	✓	–	✓	–	✓
3	–	✓	–	✓	–	✓	✓	✓
4	–	–	–	✓	✓	✓	–	✓
5	–	✓	–	✓	✓	✓	✓	✓
6	–	✓	–	✓	–	✓	–	✓
7	–	✓	–	✓	–	✓	–	✓
8	–	✓	–	✓	✓	✓	–	✓
9	–	✓	–	✓	✓	✓	✓	✓
10	–	✓	–	✓	–	–	–	–
11	–	–	–	✓	–	✓	–	✓
12	–	✓	–	✓	–	✓	–	✓
13	–	✓	–	✓	–	✓	✓	–
14	–	✓	–	✓	–	✓	–	✓
15	–	✓	–	✓	–	✓	–	✓
16	–	✓	–	✓	–	✓	–	✓
17	–	✓	–	✓	–	✓	–	✓
18	–	✓	–	✓	–	✓	✓	✓
19	–	–	–	✓	–	✓	✓	✓
20	–	–	–	✓	–	✓	–	–
Sum	0	16	0	20	4	19	6	17

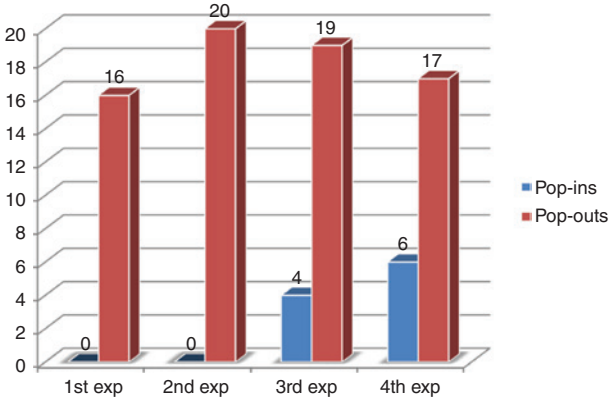

Figure 7: Bar chart of pop-ins/pop-outs in the four experiments

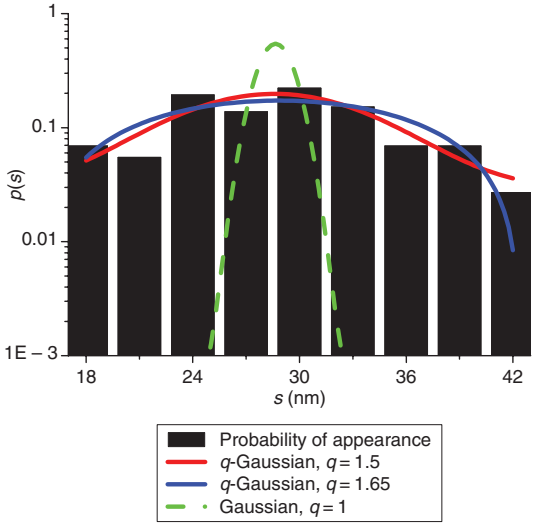

Figure 8: Probability distribution of the various pop out sizes appeared during nanoindentation procedure. The experimental data are fitted with the *q*-Gaussian probability density function.

Concerning the second phase of the investigation, we notice that in Experiment 1 with a high loading/unloading rate (80 mN/min) the amount of pop-ins was zero, while in the experiment with low loading/unloading rate (1 mN/min) the appearance of pop-in effect characterizes 75% of the number of imprints, as shown in Table 3. The above experimental results show that a low loading rate in contrast to a high favors pop-in. As it is mentioned earlier, pop-in is a distinct displacement discontinuity/jump in the loading curve. These sudden phenomena suggest that during pop-in a rapid volume shrinkage in the indentation-induced deformation zone is taking place, something that should be a result of a phase transformation from the Si-I phase to the more dense Si-II phase [3, 4]. As it is already known from the literature, a time span is required for a crystal growth like this to produce sufficient nucleation sites and to allow the crystal to grow to a certain volume, it is comprehensible that the occurrence of a pop-in is strongly connected with a slow loading rate [26].

Table 3: Table summarizing the appearance of pop-ins and pop-outs, in monocrystalline silicon for experiments with high loading/unloading rate (80 mN/min) and low loading/unloading rate (1 mN/min).

Indent number	Experiment with high loading/unloading rate		Experiment with low loading/unloading rate	
	Pop-in	Pop-out	Pop-in	Pop-out
1	–	✓	✓	✓
2	–	✓	✓	✓
3	–	✓	✓	✓
4	–	–	✓	✓
5	–	✓	–	–
6	–	✓	✓	✓
7	–	✓	✓	✓
8	–	✓	✓	✓
9	–	✓	✓	✓
10	–	✓	–	✓
11	–	–	✓	✓
12	–	✓	✓	✓
13	–	✓	–	✓
14	–	✓	–	–
15	–	✓	✓	✓
16	–	✓	✓	✓
17	–	✓	✓	✓
18	–	✓	✓	✓
19	–	–	✓	✓
20	–	–	–	–
Sum	0	16	15	17

On the other hand the number of appearance of the pop-out events remained almost the same in both experiments (17 appearances for the experiment with low loading/unloading rate and 16 appearances for the experiment with high loading/unloading rate) – see Figure 9. As we know from the literature the discontinuity in the unloading stage called pop-out, corresponds to the formation of metastable Si-XII/Si-III crystalline phases, while the hysteresis, called elbow is associated with the

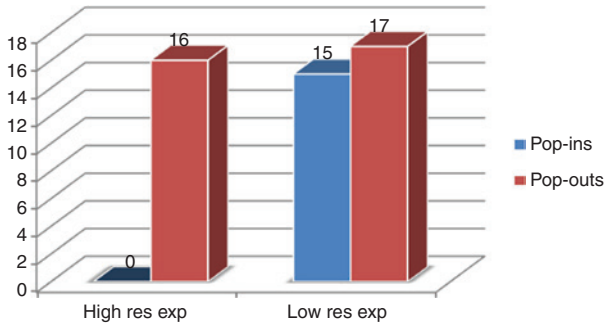

Figure 9: Bar chart of pop-ins/pop-outs in experiments with high (80 mN/min) and low (1 mN/min) indentation loading/unloading rate.

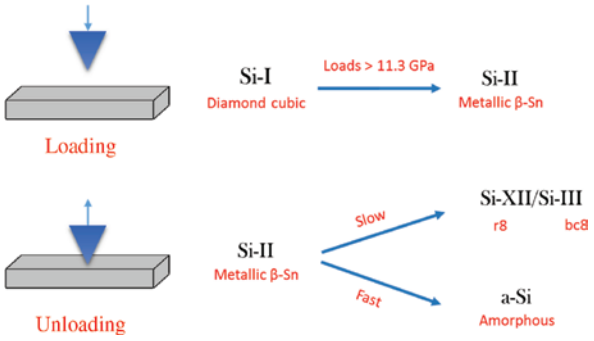

Figure 10: Phase transformations of silicon during nanoindentation procedure depending on maximum load and loading/unloading rate.

formation of amorphous Si (a-Si). It is also known that Si-II to Si-XII transformation appears to take place only when a sufficient timespan is allotted for lattice reconstruction. Rapid unloading rates favor disordering of the Si-II lattice which leads to the formation of amorphous material (a-Si), as shown in Figure 10. In our experiments we can see that in both cases the number of pop-outs remains almost the same.

As can be concluded easily from Figure 9 the appearance of pop-in events is strongly connected with the loading/unloading rate of indentation, but the appearance of pop-out effect also in this case seems to be independent of the process for the reasons we explained above.

4 Conclusions

The aim of this work was to analyze statistically the presence of the pop-in and pop-out effect during nanoindentation of monocrystalline silicon by varying the maximum applied load and loading rate.

The statistical analysis for the first set of experiments (constant loading/unloading rate, varying maximum applied load) showed that the appearance of pop-in events is strongly dependent on the maximum indentation load, while the pop-out events seem to be independent of it for the four different loads used ranging from 50 mN to 200 mN. Something which proves that we have almost always phase transformation of Si-II to crystalline phases Si-III and Si-XII during unloading for loads over 50 mN.

The statistical analysis for the second set of experiments (constant maximum load, varying loading/unloading rate) showed that the appearance of pop-in events is strongly dependent on the loading/unloading rate of indentation. On the other hand the appearance of pop-out

events also in this case seems to be independent of it (the number of pop-outs remains almost the same in both cases: ≈17 appearances in 20 experiments), something that is not expected. According to the literature rapid unloading rates favor disordering of the Si-II lattice which leads to the formation of amorphous material (a-Si), which is associated with the hysteresis of unloading curve, called elbow and not with the creation of pop-out events. These results are very interesting and must be investigated further with the use of electron microscopy.

Finally, we provided a preliminary analysis of pop-out events by using a Tsallis q-Gaussian distribution. The value of the q index observed from the fitting of the experimental data is very close to the values reported in the literature and quantifies the disorder and complexity of the systems studied in our work.

Acknowledgments: The support of the General Secretariat of Research and Technology (GSRT) of Greece through the ARISTEIA II project No. 5152, as well as the support of the Ministry of Education and Science of Russian Federation under Mega Grant Project No. 14.Z50.31.0039, is gratefully acknowledged.

References

[1] Czochralski Crystal Growth Method. Bbc.co.uk. 30 January 2003. Retrieved on 2011-12-06.
[2] Heywang W, Zaininger KH. In: Siffert P, Krimmel EF, eds. *Silicon: The Semiconductor Material*. Springer Verlag: Berlin, 2004.
[3] Jamieson JC. *Science* 1963, 139, 762–764.
[4] Hu JZ, Merkle LD, Menoni CS, Spain IL. *Phy. Rev. B* 1986, 34, 4679.
[5] Crain J, Ackland GJ, Maclean JR, Piltz RO, Hatton PD, Pawley GS. *Phy. Rev. B* 1994, 50, 13043.
[6] Piltz RO, Maclean JR, Clark SJ, Ackland GJ, Hatton PD, Crain J. *Phy. Rev. B* 1995, 52, 4072.
[7] Stone D, LaFontaine WR, Alexopoulos P, Wu TW, Li CY. *J. Mater. Res.* 1988, 3, 141–147.
[8] Pharr GM, Oliver WC, Clarke DR. *J. Electron. Mater.* 1990, 19, 881–887.
[9] Williams JS, Chen Y, Wong-Leung J, Kerr A, Swain MV. *J. Mater. Res.* 1999, 14, 2338–2343.
[10] Bradby JE, Williams JS, Wong-Leung J, Swain MV, Munroe P. *Appl. Phys. Lett.* 2000, 77, 3749–3751.
[11] Mann AB, Van Heerden D, Pethica JB, Weihs TP. *J. Mater. Res.* 2000, 15, 1754–1758.
[12] Domnich V, Gogotsi Y, Dub S. *Appl. Phys. Lett.* 2000, 76, 2214–2216.
[13] Ge D, Domnich V, Gogotsi Y. *J. Appl. Phys.* 2003, 93, 2418–2423.
[14] Bradby JE, Williams JS, Swain MV. *Phys. Rev. B* 2003, 67, 085205.
[15] Zarudi I, Zou J, Zhang LC. *Appl. Phys. Lett.* 2003, 82, 874–876.
[16] Zarudi I, Zhang LC, Cheong WCD, Yu TX. *Acta Materialia* 2005, 53, 4795–4800.
[17] Tsallis C. *J. Stat. Phy.* 1988, 52, 479–487.
[18] Oliver WC, Pharr GM. *J. Mater. Res.* 1992, 7, 1564–1583.
[19] Oliver WC, Pharr GM. *J. Mater. Res.* 2004, 19, 3–20.
[20] Arévalo R, Garcimartin A, Maza D. *Eur. Phys. J. E Soft Matter* 2007, 23, 191–198.
[21] Pavlos GP, Xenakis MN, Karakatsanis LP, Iliopoulos AC, Pavlos AEG, Sarafopoulos DV. Universality of Tsallis non-extensive statistics and fractal dynamics for complex systems, 2012. arXiv preprint arXiv:1203.5556.
[22] Tsallis C. *Introduction to Nonextensive Statistical Mechanics*. Springer: New York, 2009, pp. 37–43.
[23] Borland L. *Phys. Rev. E*, 1998, *57*, 6634.
[24] Aifantis EC. *Rev. Adv. Mater. Sci.* 2017, 48, 112–130.
[25] Aifantis EC. Internal Length Gradient (ILG) Material Mechanics Across Scales & Disciplines. 2016. arXiv preprint arXiv:1608.02383.
[26] Chang L, Zhang L. *Mater. Sci. Eng. A* 2009, 506, 125–129.